A 4D MORPHOLOGICAL SCALE SPACE REPRESENTATION FOR HYPERSPECTRAL IMAGERY

Konstantinos Karantzalos

Laboratoire de Mathematiques Appliquees aux Systemes (MAS)
Ecole Centrale de Paris, Chatenay-Malabry, France
konstantinos.karantzalos@ecp.fr

Commission VII/3

KEY WORDS: Imaging spectrometry, Mathematical morphology, Anisotropic diffusion, Image simplification, Levelings, Denoising

ABSTRACT:

In this paper, a 4D scale space representation is introduced aiming at denoising, smoothing and simplifying effectively airborne and spaceborne hyperspectral imagery. Our approach is based on a novel morphological levelings' vectorial formulation, which by integrating spatial and spectral information is able to produce elegantly simplified versions (scale spaces) of the initial hypercube. In addition, their construction is constrained by vector-valued anisotropic diffused markers which still respect the special hyperspectral data properties. In contrast to earlier efforts, under such a morphological framework the simplified scale space hypercubes are not characterized by spurious extrema or asymmetrical intensity shifts and their edges/contours are not displaced. Experimental results demonstrate the potential of our approach, indicating that the proposed representation outperforms earlier ones in quantitative and qualitative evaluation.

1 INTRODUCTION AND STATE-OF-THE-ART

Imaging spectrometry [Goetz et al., 1985] and hyperspectral sensors have experienced significant success in recent years. By offering repetitive, consistent and comprehensive data with enhanced discrimination capabilities due to their high spectral resolution, they possess a great potential for geoscience and remote sensing applications. Environmental monitoring, natural resource exploration, land-use analysis, terrain categorization, military and civil government applications for pervious/ impervious surface mapping have been much eased, while further applications in medicine, biology, pharmaceuticals, agriculture and archaeology expand the user community [Landgrebe, 2003, Maathuis and van Genderen, 2004, Schmidt and Skidmore, 2004, van der Meer, 2006, Plaza et al., 2008]. Note that for all the above applications the accuracy of the extracted information, through classification and other object detection procedures, is of major importance.

It is worth mentioning, however, that the reported average classification accuracy of remote sensing imagery is about 73% [Wilkinson, 2003] and it has not changed significantly in recent years. In addition, optimally reducing the dimensionality of hyperspectral data is still an open problem [Plaza et al., 2008]. Band selection techniques -which are not, usually, generic and may discard some bands that contain valuable information- as well as feature extraction methods -which project and may blur, the data into a low-dimensional subspace- are actually a trade-off between making the problem simpler and losing on classification accuracy [Brunzell and Eriksson, 2000, Webb, 2002]. The assumptions on the possible statistical interpretation/separation of terrain classes do not, in the general case, hold when these methods are applied directly to the initial degraded and noisy hypercube and not to an elegantly simplified version of it. Therefore, although the hyperspectral imaging market is rapidly increasing - soon with new, lighter, less expensive, higher performing generations of sensors-there still remain several challenges, regarding their multidimensional data processing, that need to be addressed [Plaza et al., 2008].

First of all, the natural variability of the material spectra, noise, physical disturbances and degradation added by the transmission media and the sensor system, reduce the separability of the different structures in hyperspectral imagery and diminish the accuracy of subsequent segmentation and classification processes. The increased significance of smaller spatial and spectral variations among pixels implies, also, that smaller amounts of noise are now likely to have a bigger impact on the results extracted from this kind of imagery. Even thought any denoising process has a significant impact on the accuracy of the results, many studies do not use any strict optimizing criteria when selecting the appropriate smoothing methods, thus, negatively affecting the outcome of subsequent analysis [Vaiphasa, 2006].

The right balance has to be found, in order to minimize not only the effect of noise but also the effect of the denoising procedure which should, moreover, take into account that objects in images appear in various scales and thus, information has to be gathered from various image scales [Lindeberg, 1994, Paragios et al., 2005]. Towards this end, Anisotropic Diffusion Filtering (ADF) has been employed for hyperspectral imagery delivering promising results in improving classification accuracy by reducing the spatial and spectral variability of images, while preserving the boundaries of the objects ([Lennon et al., 2002, Duarte-Carvajalino et al., 2007, Martin-Herrero, 2007] and there references therein). However, such a diffusion (smoothing) scale space approach, which only recently was fully adapted to the special spatial/spectral properties of hyperspectral imagery [Martin-Herrero, 2007] may reduce the problems of ad hoc inspections or isotropic filtering but does not eliminate them completely, since spurious extrema and intensity shifts may still appear [Meyer and Maragos, 2000, Karantzalos et al., 2007] (Figures 1 and 2).

Towards the same direction, other nonlinear scale-space representations, like those based on mathematical morphology, consider the evolution of curves and surfaces as a function of their geometry. Such morphological-based approaches have been, recently, proposed for processing hyperspectral imagery (e.g. [Benediktsson et al., 2005, Plaza et al., 2005]). However, conventional multiscale morphological scale-spaces like dilations and erosions (of increasing structure element size) displace objects boundaries [Jackway and Deriche, 1996]. Furthermore, the more sophisticated openings and closings by reconstruction treat image fore-
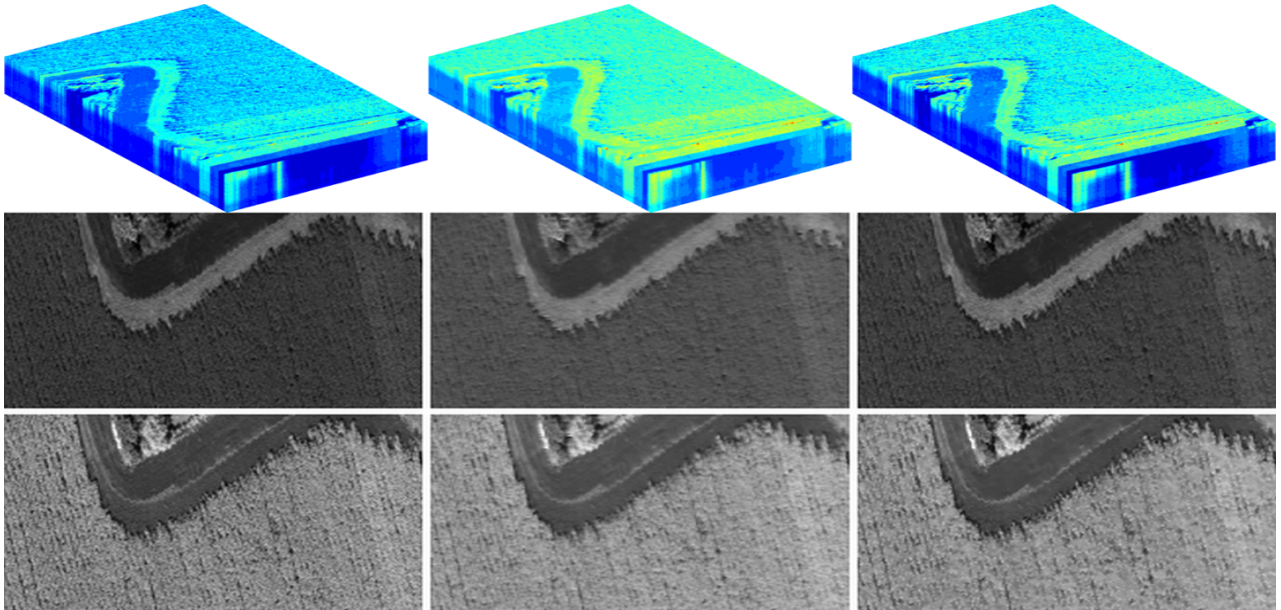
Figure 1: Smoothing and simplifying hyperspectral imagery (©Norsk Elektro Optikk). First column: A 3D view of the initial hypercube (top) and a zoom on two spectral bands i.e band number #33 (middle) and and band number #87 (bottom). Second and third columns: the resulting hypercubes and the corresponding spectral bands after anisotropic diffusion filtering ADF (second column) and after the proposed vectorial leveling AML (third). Contrary to ADF, which smoothed but created spurious extrema and intensity shifts, AML simplified and stayed constantly closer to the initial hypercube's intensity and structure.

ground (peaks) and background (valleys) in an asymmetrical manner, causing spectral shifts [Meyer and Maragos, 2000, Karantzalos et al., 2007]. Thus, they pass on these drawbacks to the succeeding classification and object detection procedures, harming their outcome significantly. A recent solution for scalar images ($\mathcal{R}^2$), came from the development of a more general and powerful class of self-dual morphological filters, the Morphological Levelings (MLs) [Meyer, 1998] which have been further studied and applied for image simplification and image segmentation by [Meyer and Maragos, 2000, Meyer, 2004].

In this paper, we aim to overcome anisotropic diffusion drawbacks and exploit all the properties that make MLs powerful. Hence, we introduce a novel 4D (the 3D hypercube plus one nonlinear diffusion scale) morphological scale space representation for denoising and simplifying hyperspectral imagery. The developed nonlinear scale space is based on the extension of the 2D morphological levelings' formulation to a multidimensional vector valued one. The novelty of our approach lies also, in the fact that our formulation takes into account the following considerations which are customized to hyperspectral data specificities, both during levelings and markers construction. The proposed vectorial scale space filtering does:

i) tackle the kind of noise that never forms a coherent structure both in spatial and spectral directions,

ii) take into account the fact that signal continuity in spectrum is, usually, more plausible than continuity in space, i.e the assumption that the spectral vector is a good approximation to the spectral signature of a particular pixel usually holds

iii) take into account the fact that object boundaries in the spatial directions should be enhanced, smoothed and elegantly simplified while their contours/edges must remain perfectly spatially localized: no edge displacements, intensity shifts or spurious extrema should occur.

Integrating spatial and spectral information while respecting the aforementioned criteria, the developed scale space morphological filtering was applied to a number of hyperspectral images and

its evaluation was carried out by both a qualitative and a quantitative assessment. The remainder of this paper is organized as follows: Starting with a brief review on conventional 2D morphological levelings in Section 2, a detailed description of the introduced vectorial extension for hyperspectral imagery is given in Section 3, along with a reference on the construction of the anisotropic markers. In Section 4, experimental results together with a discussion on the qualitative and quantitative evaluation are presented. Finally, conclusions and perspectives for future work are on Section 5. (Supplemental material can be found in http://www.mas.ecp.fr/vision/Personnel/karank/Demos/4D).

2 MORPHOLOGICAL 2D LEVELINGS

Given an image f at domain (bounded) $\Omega \in \mathcal{R}^2 \rightarrow \mathcal{R}$ and following the definitions from [Meyer, 2004, Karantzalos et al., 2007], one can consider as f_x and f_y the values of a 2D function f at pixels x and y and then define the relations: $f_y < f_x$ (f_y is lower than f_x), $f_y \geq f_x$ (f_y is greater or equal than f_x) and $f_y \equiv f_x$ (the similarity between f_x and f_y, which are at level). Based on these relations, the zones in an image without inside contours (isophotes, contour lines with constant brightness values) are called smooth/ flat zones. Being able to compare the values of neighboring pixels, a general and powerful class of morphological filters the levelling can be defined [Meyer, 1998]. MLs are a particular class of images with fewer contours than a given image f. A function g is a leveling of a function f if and only if

$$f \wedge \delta g \leq g \leq f \vee \varepsilon g \qquad (1)$$

where δ is an extensive operator ($\delta g \geq g$) and ε an anti-extensive one ($\varepsilon g \leq g$).

For the construction of MLs a class $Inter(g, f)$ of marker functions h is defined, which separates function g and the reference function f. For the function h we have that $h \in Inter(g, f)$ and so: $g \wedge f \leq h \leq g \vee f$. Algorithmically and with the use of h, one can 'interpreter' above equation and construct levelings with
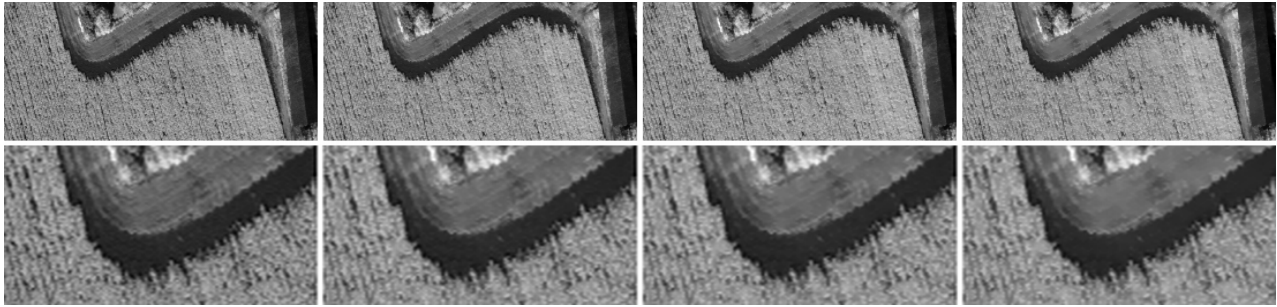
Figure 2: Simplifying hyperspectral imagery with the proposed scale space vectorial leveling (AML). First row: The initial spectral band #100 (left) and three of its increasingly simplified versions (scales $n=2, 3$ and 4). Second row: Zoom on a crop of the images above.

the following pseudo-code: in cases where $\{h < f\}$, replace the values of h with $f \wedge \delta h$ and in cases where $\{h > f\}$, replace the values of h with $f \vee \varepsilon h$. The algorithm can be repeated until the above equation has been satisfied everywhere. Its convergence is certain, since the replacements on the values of h are pointwise monotonic.This makes function g be flat on $\{g < f\}$ and $\{g > f\}$ and the procedure continues until convergence.

Under this framework MLs form a general class of morphological operators which can elegantly simplify images and possess a number of desirable nonlinear scale space characteristics. Levelings do satisfy the following properties [Meyer and Maragos, 2000, Karantzalos et al., 2007]: *i)* the invariance by spatial translation, *ii)* the isotropy, invariance by rotation, *iii)* the invariance to a change of illumination, *iv)* the causality principle, *v)* the maximum principle, excluding the extreme case where g is completely flat. In addition levelings: *vi)* do not produce new extrema at larger scales, *vii)* enlarge smooth zones, *viii)* they, also, create new smooth zones *ix)* are particularly robust (strong morphological filters) and *x)* do not displace edges. The aforementioned properties have made them a very useful simplification tool for a number of computer vision and remote sensing applications [Meyer and Maragos, 2000, Meyer, 2004, Paragios et al., 2005, Karantzalos and Argialas, 2006].

3 MULTISCALE VECTORIAL LEVELINGS FOR THE HYPERCUBE

Lets denote with $I : \Omega \subset \mathcal{R}^d \rightarrow \mathcal{R}^N$ a hyperspectral image with a normalized hyperspectrum of N spectral channels. The pseudo-scalar and autarkical vector levelings, that have been already proposed [Gomila and Meyer, 1999], are not suitable for hyperspectral imagery since they do not account for the special spatial/spectral specificities of hyperspectral data. In addition, the first ones do not efficiently enlarge flat zones and the second ones produce annoying visual artifacts due to their formulation on color propagation [Gomila and Meyer, 1999].

Excluding atmospheric effects which are tackled during a specific atmospheric correction stage, the dark or photon shot noise and the readout noise, which appears as uncorrelated high-frequency variations in the spatial and spectral space without forming a coherent structure, is what a filtering procedure should be able to address [Martin-Herrero, 2007]. However, unconstrained spatial smoothing is not desirable and in addition, spectral resolution and band adjacency are, usually, high enough to assume that the spectral vector is a good approximation to the spectral signature of the pixel, i.e the mixture of the spectral signatures of the objects within the pixel plus atmospheric, scatter and radiometric effects. Last but not least, in the spatial directions all the aforementioned in the previous section properties of the 2D levelings must be retained. To sum up a sophisticated vectorial leveling formulation

should retain all its 2D properties for the spatial directions and at the same time respect gross variations among adjacent spectral signatures and only suppress the broad spectral variations (spike-like features).

Towards this end, the levelings construction mechanism was kept the same in order to carry out the same effect on the spatial directions and reformulated in a way to include in the inequalities a comparison with the adjacent spectral signatures. Thus, the equation for the vectorial leveling takes, now, the following form:

$$f \wedge (\delta g_s \vee \delta' g_c) \leq g \leq f \vee (\varepsilon g_s \wedge \varepsilon' g_c) \qquad (2)$$

where δg_s denotes an extensive marker in the spatial axis and $\delta' g_c$ an extensive marker in the spectral one (the anti-extensive operators εg are equally defined). The spatial g_s marker acts as in the 2D case ensuring an elegant simplification in the spatial neighborhood of a pixel and the spectral g_c accounts for the spike-like features by enforcing its relevant operators (δ' and ε') to have a much broader effect. Under this framework and employing always a marker function h for levelings' construction the process is decomposed and the spectral and spatial spaces are treated differently according to the posed constrains. Rephrasing Equation (2) and in a unique parallel step we have that:

$$g = \Lambda(f, h) = \left(f \wedge (\delta h_s \vee \delta' h_c)\right) \vee (\varepsilon h_s \wedge \varepsilon' h_c) \qquad (3)$$

Hence, the proposed vectorial levelings can be considered as transformations $\Lambda(f, h)$ where a marker h is transformed to a function g, which is a leveling of the reference signal f. Where $\{(\delta h_s \vee \delta' h_c) < f\}$, h is increased as little as possible until a flat zone is created or function g reaches the reference function f and where $\{(\varepsilon h_s \wedge \varepsilon' h_c) > f\}$, h is decreased as little as possible until a flat zone is created or function g reaches the reference function f. This process simplifies the hypercube by enlarging and by creating new flat zones and this procedure continues until convergence.

3.1 Scale Space Hypercubes

Hyperspectral data can be viewed like any video data, where the wavelength corresponds to time or like MRI volumes in medical imaging, where wavelength corresponds to another spatial axis. Instead of defining the stack of a hyperspectral image as $I : \Omega \subset \mathcal{R}^d \rightarrow \mathcal{R}^N$, where N is the number of spectral channels and $I = (I_1(x, y), ..., I_N(x, y)) \in \mathcal{R}^N$, a hypercube can be defined, also, as a 3D function $\mathcal{I} : \Omega \subset \mathcal{R}^3 \rightarrow \mathcal{R}$, where $\mathcal{I}(x, y, z) = I_z(x, y)$.

Following this notation, multiscale levelings can be constructed when the initial (reference) hypercube $\mathcal{I}$ is associated with a series of marker functions $\{h_1, h_2, ..., h_n\}$ -all h are increasingly
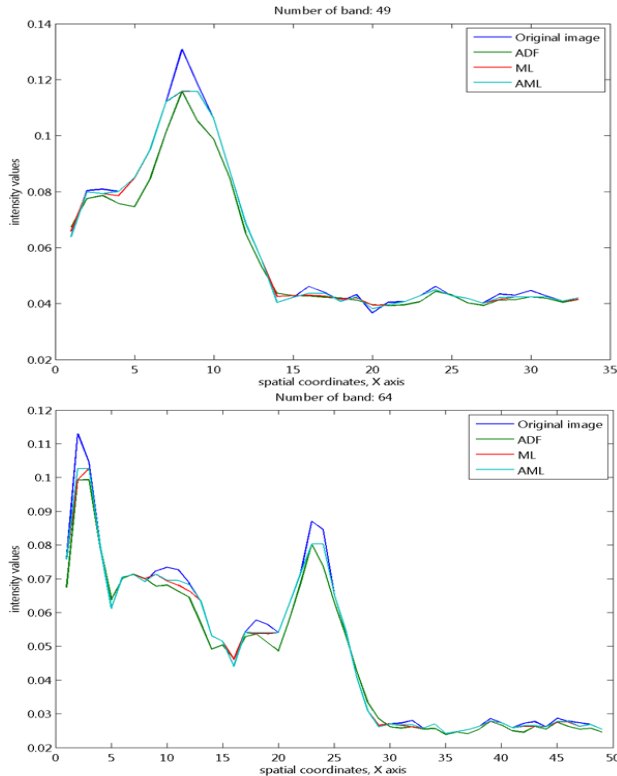
Figure 3: Spatial simplification: Comparing the filtering result of ADF, ML (channel by channel process) and the proposed vectorial AML. Two line plots with the cross-sections along the y-axis of the different filters are shown for bands #49 (top) and #64 (down). The proposed AML did simplify the initial image by enlarging and creating new flat zones and at the same time followed more constantly and closely original image's intensity values and variation. AML did retain all its elegant 2D properties.
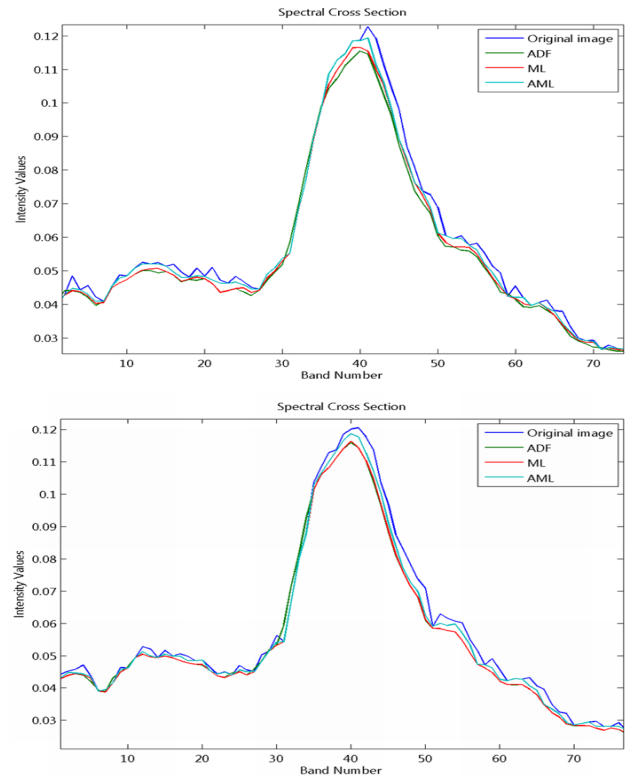

Figure 4: Spectral simplification: Comparing the filtering result of ADF, ML and AML. Two line plots with the cross-sections along the spectral axis of the different filtered hypercubes are shown. The proposed AML did surpassed broad spectral variations (spike-like features) among adjacent spectral signatures and at the same time followed more constantly the initial intensity.

smoother hypercubes in $\mathcal{R}^3$. The constructed levelings are respectively

$$g_1 = \mathcal{I}, \ g_2 = \Lambda(g_1, h_1), \ g_3 = \Lambda(g_2, h_2), \\ g_4 = \Lambda(g_3, h_3) \ ,..., \ g_n = \Lambda(g_{n-1}, h_{n-1}) \tag{4}$$

A series g_n of simpler and simpler hypercubes, with fewer and fewer smooth zones are produced forming a 4D scale space with $g : \Omega \subset \mathcal{R}^4$ and $g(x, y, z, n) = g_n(x, y, z)$. Similar to the 2D case the introduced, here, vectorial morphological levelings AMLs can be associated to an arbitrary or an alternating family of marker functions. Examples with openings, closings, alternate sequential filters and isotropic and anisotropic markers can be found in the literature for scalar images [Meyer, 1998, Meyer and Maragos, 2000, Meyer, 2004, Karantzalos et al., 2007]. For specific tasks one may take advantage of the possible prior knowledge for scene's content and design accordingly the family of markers.

3.2 Anisotropic Diffused Markers

For the construction of the simplified hypercubes anisotropic diffused markers were chosen, since they have proven to be effective for scalar images [Karantzalos et al., 2007]. In addition, since levelings are highly constrained by the type of the marker used [Meyer and Maragos, 2000], only those markers who are fully suitable for hyperspectral imagery were appropriate for our case. The recent formulations of [Martin-Herrero, 2007] provide a suitable diffusion framework which respects the special characteristics of hyperspectral data by separating the elegant vector-

valued diffusion approach of [Tschumperle and Deriche, 2005] in the spatial and spectral space. For a hypercube $\mathcal{I} : \Omega \subset \mathcal{R}^3$ the anisotropic diffusion process is expressed by the following equation:

$$\frac{\vartheta \mathcal{I}}{\vartheta t} = \text{trace}(TH) \tag{5}$$

with H and T the 3x3 Hessian and diffusion tensor matrices, respectively. The tensor separates the diffusion in the spatial and spectral directions while suitable edge-stoping functions r_i control the diffusion:

$$T = r_x \theta_+ \theta_+^T + r_y \theta_- \theta_-^T + r_z zz^T \tag{6}$$

with θ the eigenvectors of a 2x2 metric tensor D which depends on the spatial derivatives:

$$D = G_\sigma * \sum_i^N \nabla I_i \nabla I_i^T \tag{7}$$

where G_σ is a gaussian smoothing for regularizing the spatial 2D derivatives of ∇I at every channel N. In [Martin-Herrero, 2007] the edge stoping functions r_i, which act differently in the spatial and spectral directions, have been defined in such a way so as to allow all possible adjustments regarding their regularization effect. One should tune all the coefficients according to image characteristics and the filtering purpose. For a scale space representation, however, where

$$\mathcal{I} : \Omega \subset \mathcal{R}^4, \ \mathcal{I}(x, y, z, n) = \mathcal{I}_n(x, y, z) \tag{8}$$

(n is the scale of diffusion) one may avoid tuning the vector edge strength $r_i(v)$ -with $v = \sqrt{\text{trace}(D)}$- and rely on the
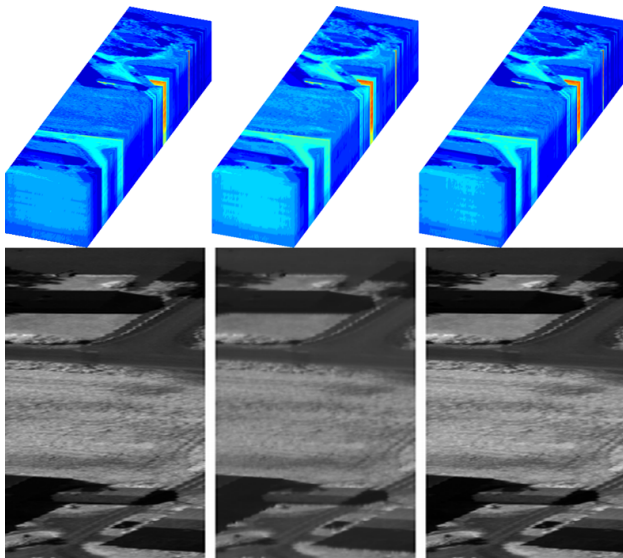
Figure 5: Smoothing and simplifying hyperspectral imagery (©Norsk Elektro Optikk). First column: A 3D view of the initial hypercube (top) and a zoom on the band number #94 (middle). Second and third column: the resulting hypercubes and the corresponding bands after applying the ADF (second column) and the proposed AML (third column). Contrary to ADF, which smoothed without preserving image flat zones, AML simplified and stayed constantly close to the initial hypercube intensity values and structure.

adaptive time step $\Delta t = \Delta \mathcal{I}_{max}/max(|\text{trace}(\text{TH})|)$ or on another selected one. In cases where just a single simplified hypercube is needed, the coefficients can be customized accordingly. The proposed, thus, vectorial leveling AML takes its final form when in Equation (4) the family of markers h_n are derived from the anisotropic diffused markers $\mathcal{I}_n$ of Equation (8). Such anisotropic markers, which do respect hyperspectral data specificities, can naturally ameliorate the simplification process, without, in addition, demanding a search for selecting the appropriate structure element size and type, as the classical morphological operators do.

4 EXPERIMENTAL RESULTS - EVALUATION

The developed vectorial Anisotropic Morphological Leveling AML was applied to a number of hyperspectral images and its evaluation was carried out by both a qualitative and a quantitative assessment. Datasets from the HySpex VNIR-1600 airborne sensor (©Norsk Elektro Optikk A/S) with 160 channels (400-1000nm), from the CASI-1500 airborne sensor (©ITRES) with 36 channels (380-1050nm) and from EOS-1 Hyperion (©USGS) spaceborne sensor with 220 channels were available. Throughout the evaluation procedure the compared ADF was the same with the one that was used for the construction of the AML and each scale n was derived after three iterations t. Both were also compared with the classical ML after a standard channel by channel process to the resulting ADF hypercube. For the quantitative evaluation apart from the standard RMSE and NMSE measures -which give a quantitative sense for the extent of variation between the intensity values of the compared images- the recently proposed complementary quality measure of SSIM [Wang et al., 2004] was, also, employed because it is able to compare effectively local patterns of pixel intensities under a perceived visual quality. The lower RMSE and NMSE and the bigger SSIM values designate the better filtering result.

Table 1: Quantitative Evaluation

Test Data	Type of Filter	Quantitative Measures		
		RMSE	NMSE	SSIM
Figure 1 Hypercube	ADF	0.012	0.009	0.996
	ML	0.009	0.004	0.998
	AML	0.006	0.002	0.999
Figure 1 Band #33	ADF	0.097	0.156	0.985
	ML	0.035	0.020	0.996
	AML	0.034	0.018	0.998
Figure 1 Band #87	ADF	0.068	0.021	0.944
	ML	0.055	0.013	0.974
	AML	0.049	0.011	0.974
Figure 2 Band #100	ADF	0.147	0.093	0.982
	ML	0.049	0.010	0.997
	AML	0.041	0.007	0.998
Figure 5 Hypercube	ADF	0.009	0.004	0.998
	ML	0.004	0.001	0.999
	AML	0.003	0.001	1.000
Figure 5 Band #94	ADF	0.052	0.018	0.973
	ML	0.025	0.005	0.992
	AML	0.020	0.003	0.995
Noisy Hypercube	ADF	0.013	0.012	0.996
	ML	0.009	0.007	0.997
	AML	0.008	0.004	0.998

In Figure 1, 3D views of the initial hypercube and the resulting ones from the ADF and the AML are presented, together with two corresponding bands #33 and #87 (filtering scale n=3). The ADF smoothed strongly the data and created some intensity shifts. In contrast the AML simplified the data but kept a closer relation with the initial hypercube intensity values. This can be more clearly verified by a close look at Figures 3 and 4, where cross sections along the spatial y-axis and the spectral axis are presented, respectively. One can observe that even thought all the compared filters did not displace edges, the AML almost everywhere stayed closer to the initial hypercube. AML simplified the image in the spatial directions by enlarging or creating new flat zones (levelled regions with constant intensity values), retaining all its 2D scale space properties. In the spectral direction it accounted for large intensity variations (spike-like features) and at the same time stayed close to the initial hypercube values. The above observations can be further confirmed by the performed quantitative evaluation (Table 1). In all cases (Figure 1), the AML resulted to the lower RMSE and NMSE values and to the larger structural similarity with the original image (SSIM).

In Figure 2, the initial and three of the resulting AML scale space images are presented (scales n=2, 3 and 4). The increasingly simplified versions of the original spatial image structure can be observed. The quantitative comparison between AML's result (at scale n=4) with the corresponding ML and ADF (Table 1), indicate that the AML scored better in all measures. Furthermore and evaluating the compared filtering techniques in another dataset (shown in Figure 5), approximately the same conclusions were derived. In Figure 5, 3D views of the initial hypercube and the ones resulting from the ADF and the AML are shown, together with the corresponding band #94. By comparing qualitatively, all filtering results in the same scale (n=6), it can be observed that the difference between diffusing (smoothing with ADF) and simplifying (AML) adjacent intensity variations, is that a more elegantly enhanced version of the original image is obtained from the AML. Both methods respect image edges but the proposed AML enforces the creation of flat regions instead of diffusing inside them. This process obliges, also, AML to follow more constantly the original hypercube's intensity. The above observations can be confirmed by the quantitative measures in Table 1 which indicate that the AML scored better in all measures,

in terms of keeping the extent of intensity variation (RMSE and NMSE) small and the structural similarity (SSIM) with the reference hypercube high. Such elegantly simplified data can be used instead of the original noisy ones, improving the performance of the succeeding band selection, feature extraction and classification procedures, especially the unsupervised ones. The AML, naturally, provides a simpler space for statistical modeling and interpretation, by preserving distinguishable data features while reducing spatial and spectral intensity variation.

Moreover, the compared filtering techniques were applied in removing noise from an artificially contaminated hypercube. One percent of the original hypercube's pixels were contaminated with uncorrelated noise and then ADF, ML and AML of scale n=6 were applied. The quantitative measures when comparing results with the original hypercube are presented in Table 1. The developed AML scores better in all measures approximating successfully the original hypercube's intensity and structure. Last but not least, the AML was tested against watershed's over-segmentation problem. In all performed experiments, a reduction of over a 10% was achieved to the number of the output segments. AML managed to decrease the heterogeneity of the initial image (both in spectral and spatial directions) by merging pixels which belonged to the same object/class, impelling the sensitive watershed transformation to result in fewer output segments.

5   CONCLUSIONS

We have introduced a novel morphological scale space representation for denoising and simplifying hyperspectral data. Experimental results and performed quantitative evaluation demonstrate that the developed AML can enlarge and create new flat zones without displacing image contours and can surpass spectral spike-like features outperforming anisotropic diffusion filtering and standard MLs. The algorithm is relative fast and without an optimized coding, can approximately process a hypercube of 200x350 pixels with 160 channels in less than a minute (for every scale n) in an ordinary iPentiumM 2GHz,1GB RAM. For real-time applications its implementation on a parallel system is straightforward and furthermore, the algorithm can be adjusted and do not process the thermal infrared bands, other heavily noised or selected ones. The suitable for hyperspectral data morphological framework, the resulting, in all our experiments, elegant simplification and the adequate algorithm's performance encourage future research. Object-oriented hyperspectral image analysis, where the multiscale segmentation and classification is constrained by the developed AML is currently under investigation.

REFERENCES

Benediktsson, J. A., Palmason, J. A. and Sveinsson, J. R., 2005. Classification of hyperspectral data from urban areas based on extended morphological profiles. IEEE Transactions on Geoscience and Remote Sensing 42, pp. 480–491.

Brunzell, H. and Eriksson, J., 2000. Feature reduction for classification of multidimensional data. Pattern Recognition 33, pp. 1741–1748.

Duarte-Carvajalino, J., Castillo, P. and Velez Reyes, M., 2007. Comparative study of semi-implicit schemes for nonlinear diffusion in hyperspectral imagery. IEEE Transactions on Image Processing 16, pp. 1303–1314.

Goetz, A. F. H., Vane, G., Solomon, J. E. and Rock, B. N., 1985. Imaging spectrometry for earth remote sensing. Science 228, pp. 1147–1153.

Gomila, C. and Meyer, F., 1999. Levelings in vector spaces. In: IEEE International Conference on Image Processing, Vol. 2, Kluwer Academic, pp. 929–933.

Jackway, P. T. and Deriche, M., 1996. Scale-space properties of multiscale morphological dilation-erosion. IEEE Transactions on Pattern Analysis and Machine Intelligence 18(1), pp. 38–51.

Karantzalos, K. and Argialas, D., 2006. Improving edge detection and watershed segmentation with anisotropic diffusion and morphological levelings. International Journal of Remote Sensing 27, pp. 5427–5434.

Karantzalos, K., Argialas, D. and Paragios, N., 2007. Comparing morphological levelings constrained by different markers. In: ISMM, G.Banon, et al. (eds), Mathematical Morphology and its Applications to Signal and Image Processing, pp. 113–124.

Landgrebe, D. A., 2003. Signal theory methods in multispectral remote sensing. Hoboken: John Wiley and Sons.

Lennon, M., Mercier, G. and Hubert-Moy, L., 2002. Classification of hyperspectral images with nonlinear filtering and support vector machines. In: IEEE International Geoscience and Remote Sensing Symposium, Vol. 3, pp. 1670–1672.

Lindeberg, T., 1994. Scale-Space Theory in Computer Vision. Kluwer Academic Publishers, Dordrecht.

Maathuis, B. and van Genderen, J., 2004. A review of satellite and airborne sensors for remote sensing based detection of minefields and landmines. International Journal of Remote Sensing 25(23), pp. 5201–5245.

Martin-Herrero, J., 2007. Anisotropic diffusion in the hypercube. IEEE Transactions on Geoscience and Remote Sensing 45, pp. 1386–1398.

Meyer, F., 1998. From connected operators to levelings. In: Mathematical Morphology and Its Applications to Image and Signal Processing, (H. Heijmans and J. Roerdink, Eds.), Kluwer Academic, pp. 191–198.

Meyer, F., 2004. Levelings, image simplification filters for segmentation. International Journal of Mathematical Imaging and Vision 20, pp. 59–72.

Meyer, F. and Maragos, P., 2000. Nonlinear scale-space representation with morphological levelings. Journal of Visual Communication and Image Representation 11, pp. 245–265.

Paragios, N., Chen, Y. and Faugeras, O., 2005. Handbook of Mathematical Models of Computer Vision. Springer.

Plaza, A., Benediktsson, J. A., Boardman, J., Brazile, J., Bruzzone, L., Camps-valls, G., Chanussot, J., Fauvel, M., Gamba, P., Gualtieri, A., Marconcini, M., Tilton, J. and Trianni, G., 2008. Recent advances in techniques for hyperspectral image processing. Remote Sensing of Environment,(to appear).

Plaza, A., Martinez, P., Plaza, J. and Perez, R., 2005. Dimensionality reduction and classification of hyperspectral image data using sequences of extended morphological transformations. IEEE Transactions on Geoscience and Remote Sensing 43, pp. 466–479.

Schmidt, K. and Skidmore, A., 2004. Smoothing vegetation spectra with wavelets. International Journal of Remote Sensing 25(6), pp. 1167–1184.

Tschumperle, D. and Deriche, R., 2005. Vector-valued image regularization with pdes: A common framework for different applications. IEEE Transactions on Pattern Analysis and Machine Intelligence 27(4), pp. 506–517.

Vaiphasa, C., 2006. Consideration of smoothing techniques for hyperspectral remote sensing. International Journal of Photogrammetry and Remote Sensing 60, pp. 91–99.

van der Meer, F., 2006. The effectiveness of spectral similarity measures for the analysis of hyperspectral imagery. International Journal of Applied Earth Observation and Geoinformation 8(1), pp. 3–17.

Wang, Z., Bovik, A., Sheikh, H. and Simoncelli, E., 2004. Image quality assessment: From error visibility to structural similarity. IEEE Transactions on Image Processing 13, pp. 600–612.

Webb, A., 2002. Statistical Pattern Recognition. John Wiley and Sons Ltd., UK.

Wilkinson, G., 2003. Are remotely sensed image classification techniques improving? Results of a long term trend analysis. In: IEEE Workshop on Advances in Techniques for Analysis of Remotely Sensed Data, Greenbelt, Maryland, pp. 27–28.